Erratum
December 18, 2018. DOI: 10.1159/000496123

Cellular Physiology and Biochemistry

Cell Physiol Biochem 2018;50:987-1004
DOI: 10.1159/000494482
Published online: 23 October 2018
Accepted: 15 October 2018

Original Paper

Downregulation of N-Acetylglucosaminyltransferase GCNT3 by miR-302b-3p Decreases Non-Small Cell Lung Cancer (NSCLC) Cell Proliferation, Migration and Invasion

Qian Li[a,b] Pengzhan Ran[a] Xiyu Zhang[a] Xiaopeng Guo[a] Yuncang Yuan[a] Tianqi Dong[a] Bei Zhu[a] Shangyong Zheng[a] Chunjie Xiao[a]

[a]School of Medicine, Yunnan University, Kunming, [b]Transfusion Medicine Research Department,Yunnan University, Kunming, China

Key Words
Nsclc • GCNT3 • miR-302b-3p • RNA sequencing • miRIP • Tumorigenesis

Abstract
Background/Aims: GCNT3 is a member of N-acetylglucosaminyltransferase family involved with mucin biosynthesis. GCNT3 aberrant expression is known to promote the progression of several human cancers. However, its role in tumorigenesis and the progression of non-small cell lung cancer (NSCLC) has not been well-characterized. Our study investigated the functional mechanisms of GCNT3 regulated by microRNAs (miRNAs) in NSCLC. ***Methods:*** The differential expression of mRNAs in NSCLC tissues and matched adjacent non-cancerous lung tissues from patients in Xuanwei, Yunnan province, China, was screened via mRNA microarray. The expression of GCNT3 and its correlation with NSCLC progression was measured in 92 paired tumor tissues and adjacent normal tissues. The functions of GCNT3 in NSCLC cells and its underlying mechanisms were measured using siRNA and GCNT3-expression vectors. The miRNA immunoprecipitation (miRIP) method was used to identify the miRNAs targeting GCNT3. The protein were measured using western blot assay, and the mRNAs were measured by quantitative real-time PCR (qRT-PCR) assay. Cell proliferation was measured using Cell Counting Kit-8 (CCK-8) and a colony forming assays; cell migration and invasion assays were performed using 24-well Transwell chambers with 8-μm pores filter, and analyses of the cell cycle and apoptosis were performed via flow cytometric analysis. The dual luciferase reporter assay was performed to confirm whether GCNT3 gene was a direct target of miR-302b-3p. ***Results:*** GCNT3 was found to be highly expressed in both NSCLC tissues and cell lines, and higher expression correlated significantly with advanced tumor-node-metastasis (TNM) stage, positive lymph node metastasis, and poor overall survival. Knockdown of GCNT3 inhibited the

Q. Li, P. Ran and X. Zhang contributed equally to this work.

Chunjie Xiao
and Shangyong Zheng

School of Medicine, Yunnan University
Yunnan 650091 (China)
E-Mail chunjiexiaoynu@126.com; shangyong@ynu.edu.cn

proliferation, migration and invasion ability of NSCLC cells, while overexpression facilitated these activities. Further mechanistic experiments using miRIP and dual luciferase reporter assays revealed that GCNT3 was a direct target of miR-302b-3p. Low expression of miR-302b-3p was found in NSCLC cells and negatively correlated with GCNT3 levels, while miR-302b-3p overexpression inhibited the proliferation, migration and invasion of NSCLC cells. Co-transfection with miR-302b-3p and the expression vector of GCNT3 abrogated the effects of mir-302b-3p, confirming that miR-302b-3p inhibited NSCLC progression by targeting GCNT3. Western blotting revealed that E-cadherin, N-cadherin, vimentin, p-Erk and cyclin D1 were downstream molecules of miR-302b-3p/GCNT3 pathway. ***Conclusion:*** miR-302b-3p/GCNT3 axis regulated cell proliferation, migration, and invasion by activating the Erk signaling pathway and epithelial-mesenchymal transition (EMT), which was identified as a potential therapeutic target for NSCLC.

Introduction

Lung cancer is the most commonly diagnosed malignancy [1, 2], and more than 80% of patients with lung cancer are diagnosed with NSCLC[3]. In Yunnan Province, especially in Xuanwei City, the incidence of NSCLC is ranked the highest in world [4]. A mortality survey, conducted in Xuanwei during 2004–2005, revealed that the average mortality rate in NSCLC was 91.3 per 100, 000 in Xuanwei City [5], and the age at onset of lung cancer was 15–25 years younger than the average age in China [5]. Another survey, conducted in Xuanwei during 2011–2013, indicated that the male and female mortality rates in NSCLC were three and six times higher, respectively, in this region than in rural areas of China [6]. Due to these factors, NSCLC occurring in this area is known as Xuanwei Lung Cancer (XWLC). Even in the past few decades, despite the latest developments in NSCLC diagnosis and therapeutics, the overall survival (OS) rate of NSCLC patients still remains poor [7]. Therefore, it is essential to identify novel biomarkers with high specificity and sensitivity to increase the effectiveness of diagnostic, prognostic, and therapeutic strategies for NSCLC.

O-Glycan synthesis enzyme glucosaminyl (N-acetyl) transferase 3, mucin type (GCNT3/GNTM/C24GNT/C2GNT2/C2GNTM/C2/4GnT) is on human chromosome 15q22.2 and encodes a member of the N-acetylglucosaminyltransferase family, which catalyzes the formation of core 2 and core 4 O-glycans on O-linked glycosylation in mucin biosynthesis [8]. Cancer cells develop abnormal accumulation of mucin that covers epithelial cells and hinders drug access, which leads to cancer chemoresistance [9]. Recent research has shown that GCNT3 promotes human tumorigenesis. Rao et al. (2016) reported that GCNT3 is significantly overexpressed in human pancreatic cancer, and high GCNT3 expression is associated with the smoking and drinking habits of patients, as well as a diagnosis of diabetes [10]. GCNT3 has also been found to be under-expressed in stage II colon tumors compared with human normal colon tissues [11]. Moreover, GCNT3 gene is probably involved in the immunotoxicity, teratogenicity, and disruption of lipid metabolism caused by polycyclic aromatic hydrocarbons [12]. However, little is known about the role of GCNT3 in NSCLC, especially in XWLC, and its biological function and clinical significance has not yet been established.

MicroRNA (miRNAs) regulate a broad range of cellular processes, including cell growth, proliferation and apoptosis, through post-translational modulation of their targets [13]. We focused on miR-302b-3p in this study, because it has been confirmed – through a new method known as miRNA immunoprecipitation (miRIP) assay, established by Xiaoping Su – that it targets GCNT3 [14]. MiR-302b is a promising biomarker and candidate therapeutic target for multiple types of human cancers [15-17]. It has been found to sensitize breast cell lines in cisplatin treatment [15], suppress cell proliferation in hepatocellular carcinoma [16], and induce apoptosis in epithelial ovarian carcinoma [17]. Therefore, it is of great importance to clarify the regulatory pattern between GCNT3 and miR-302b-3p during NSCLC tumorigenesis.

In this study, GCNT3 was found via mRNA microarray to be up-regulated in NSCLC tissues compared with adjacent noncancerous tissues. qRT-PCR and western blot analysis demonstrated that GCNT3 was overexpressed in both NSCLC cancer cell lines (XWLC and NCI-H292) and primary lung cancer tissues from patients in Xuanwei, Yunnan Province, China. Knockdown of GCNT3 inhibited NSCLC cell proliferation, migration and invasion, while GCNT3 overexpression promoted these activities. miRIP and dual_luciferase reporter gene assays showed that miR-302b-3p could target GCNT3. The modulatory pattern between GCNT3 and miR-302b-3p and its role in XWLC tumorigenesis was investigated in NSCLC cells. GCNT3 was found to be a target of miR-302b-3p and enabled miR-302b-3p to participate in the pathogenesis and progress of NSCLC. Moreover, western blot experiments revealed that E-cadherin, N-cadherin, vimentin, cyclin D1 and p-Erk were downstream molecules of the miR-302b-3p/GCNT3 pathway. Our results indicated that GCNT3, negatively controlled by miR-302b-3p, regulated proliferation, migration and invasion in NSCLC cells by facilitating the activation of the ERK signaling pathway and EMT, which could be a potential biomarker for NSCLC diagnosis and therapy.

Materials and Methods

Collection of specimens and clinical data

This study was approved by the Ethics Committee of School of Medicine Yunnan University, and performed in accordance with the standards set by the Declaration of Helsinki. Written informed consent was obtained from each subject before participation in this study. All samples of NSCLC tissues and adjacent non-tumor tissues were collected from patients undergoing surgical procedures at the Third Affiliated Hospital of Yunnan Kunming Medical University. Only samples from NSCLC patients who had not undergone operative chemotherapy, radiotherapy, or targeted therapy were collected. Among them, 15 pairs of NSCLC and adjacent non-cancerous lung tissue samples obtained during surgery were snap-frozen immediately in liquid nitrogen, and stored at –80°C until further processing to avoid degradation of the RNA. Another 92 pairs of NSCLC and adjacent non-cancerous lung tissues were paraffin-embedded. The clinicopathological features of the patients were collected from medical records and were summarized in Table 1. Tumor staging was based on the seventh edition of the Union for International Cancer Control (UICC) TNM staging system for lung cancer [18]. All 92 NSCLC cases underwent follow-up via telephone, and the OS rate of each patient was calculated from the time of the initial surgery to the end of follow-up or the day of death.

Table 1. Correlation between GCNT3 expression and clinicopathologic parameters in NSCLC Patients (n=92). Note: TNM, tumor-node-metastasis staging system; P values were calculated using chi-square test; *p < 0.05, **p < 0.01

Clinical characteristics	Total number	GCNT3 expression		p-value
		Low(n=37)	High(n=55)	
Age				
<55	21	9	12	0.7788
≥55	71	28	43	
Gender				
Male	51	19	32	0.5181
Female	41	18	23	
Tumor size				
<5cm	72	30	42	0.5906
≥5cm	20	7	13	
TNM stage				
Stage I/II	57	29	28	0.0078**
StageIII/IV	35	8	27	
Lymph node metastasis				
Negative	39	23	16	0.0016**
Positive	53	14	39	
Survival years after surgery				
<3 year	47	12	35	0.0033**
≥3 year	45	25	20	

Cell lines

Two human NSCLC cell lines (A549 and NCI-H292) and a human normal pulmonary epithelial cell line (BEAS-2B) were purchased from American Type Culture Collection (Manassas, VA), and another two local NSCLC cell lines (XWLC and GLC) were isolated from the cancer tissues of patients lived in Xuanwei, a region in the Yunnan Province of China. Among them, A549, GLC and XWLC cell lines were cultured in Dulbecco's modified Eagle's medium (DMEM, HyClone, Logan, UT) medium containing 10% fetal bovine serum (HyClone) and 1% penicillin and streptomycin (Life Technologies, Carlsbad, CA), while NCI-H292 and BEAS-2B cell lines were maintained in RPMI 1640 (HyClone) medium with 10% fetal bovine serum (HyClone) and 1% penicillin and streptomycin (Life Technologies), at 37°C in a humidified air atmosphere containing 5% CO_2.

Human Gene Expression Microarray assay

Total RNA from 15 pairs of NSCLC and adjacent non-cancerous lung tissues were isolated using the TRIzol agent (Invitrogen, Carlsbad, CA) following the manufacturers' instruction. The quality of RNA samples was tested via the NanoDrop2000 (Thermo-Fisher Scientific, Waltham, MA, USA). Analysis of the expression profile of NSCLC-related genes was performed by a commercially available oligonucleotide microarray (Affymetrix GeneChip Human Transcriptome Array 2.0, Thermo Fisher Scientific) following the manufacturer's recommendations. The array images were further analyzed by Agilent Feature Extraction software (version_10.7.1.1, Agilent Technologies, Santa Clara, CA). The raw data were normalized using the quantile algorithm. Differentially expressed genes were then identified through fold changes, and the *P* values were calculated with the Student's t-test. The threshold values set for up- and down-regulated genes was a fold change ≥ 2.0 and a *P* value<0.05.

Immunohistochemistry (IHC)

GCNT3 protein expression was assessed by immunohistochemistry (IHC) in 92 pairs of NSCLC and adjacent non-cancerous lung tissue sections. Tissues were fixed in 10% neutral formalin and embedded in paraffin. The paraffin-embedded NSCLC specimens were sliced into 4–μm–thick sections. Sections were then deparaffinized with xylene and rehydrated with a graded series of ethyl alcohol. Antigen retrieval was achieved by microwave treatment in 0.01 M sodium citrate buffer (pH 6.0) for 10 min. Endogenous peroxidase was inactivated by treatment with 0.3% hydrogen peroxide for 10 min. Tissue sections were heated for 5 min at 121°C and then cooled to 85°C. To prevent non-specific binding, we blocked the sections with goat serum (BioGenex, San Ramon, CA) for 30 min at room temperature. We then incubated the sections with anti-GCNT3 (TA332087, 1:50, Origene, Rockville, MD) at 4°C overnight, followed by biotinylated goat anti rabbit IgG secondary antibody. For the negative control (NC), sections were treated with phosphate-buffered saline (PBS) instead of antibody. After washing, immunoreactivity was developed using diaminobenzidine tetrahydrochloride (DAB) solution (Vector Laboratories, Burlingame, CA). Tumor specimens were then counterstained with hematoxylin, dehydrated in alcohol, and mounted. The scores were calculated by evaluating the staining intensity and percentage of stained cells in representative areas via two investigators blinded to the clinical parameters. The expression score in IHC, defined as the staining intensity multiplied by the percentage of tumor positive area, was semi-quantitatively determined by the H-score (0–300). A median value derived from the testing set and applied to the validation set determined the cut-off point for tumoral GCNT3 high/low-level expression. The cut-off point was set at 75.

RNA extraction and quantitative real-time PCR (qRT-PCR) assays

Total RNA was extracted from NSCLC specimens or cultured cells by TRIZOL reagent (Invitrogen, Carlsbad, CA) following the manufacturer's instructions and treated with DNase I (Invitrogen, Carlsbad, CA) to eliminate potential DNA contamination. The extracted RNA was reverse-transcribed into cDNA by using a Reverse Transcription Kit (Takara, Dalian, China) according to the manufacturer's protocol. Quantitative real-time PCR (qRT-PCR) was performed with SYBR Premix Ex Taq (Takara, Dalian) on a CFX96 Touch™ Real-Time PCR Detection System (Bio-Rad Laboratories, Hercules, CA), and the data were collected. The mRNA transcription levels were normalized to the expression of GAPDH, and the miRNA transcription levels were normalized to the expression of U6. The sequences of the primers were as follows: GCNT3 (forward:5′-GCCAGTAAGCTGGTTCGG-3′, reverse:5′-GCCAGTAAGCTGGTTCGG-3′), GAPDH (forward: 5′-GACAGTCAGCCGCATCTTCT-3′, reverse: 5′-TTAAAAGCAGCCCTGGTGAC-3′), miR-302b-3p (loop:

5′-GTCGTATCCAGTCCAGGGACCGAGGACTGGATACGACCTACTA-3′, forward: 5′-GCGTAAGTGCTTCCATGTT-3′, reverse: 5′-TCCAGGGACCGAGGA-3′) and U6(loop: 5′-CGCTTCACGAATTTGCGTGTCAT-3′, forward: 5′-GCTTCGGCAGCACATATACTAAAAT-3′, reverse 5′-CGCTTCACGAATTTGCGTGTCAT-3′.). The expression levels of the genes of interest, GCNT3 or miR-302b-3p, were relative to the threshold cycle (CT) values, and converted to fold changes. All experiments were conducted in triplicate.

Plasmid generation and transfection

The full-length GCNT3 sequence was synthesized by Beijing Genomics Institute (Beijing, China) and subcloned into the pEX-3 vector (GenePharma, Shanghai, China) to generate the pEX-3-GCNT3 following the manufacturer's instructions. An empty pEX-3 vector was used as a control. The recombinant plasmids were extracted by Pure Yield™ Plasmid Midiprep kit (Promega Corp., Madison, WI) and sequenced (Sain Biological Corporation, Shanghai, China). pEX-3-GCNT3 and empty pEX-3 plasmids (5μg plasmid DNA) were transfected into NSCLC cells using Lipofectamine® 3000 Reagent (Thermo Fisher Scientific) in a 6-well cell culture plate according to the manufacturer's instruction, respectively. Cells were harvested 48 hours after transfection, to detect overexpression or for further functional assays.

Small interfering RNA and miRNA transfection

For RNAi-mediated knockdown of GCNT3, small interfering RNAs (siRNAs) specific to GCNT3 (GCUACUGCGAGCUGUGUAUTT) and a control siRNA (UUCUCCGAACGUGUCACGUTT) were designed and synthesized by GenePharma (shanghai, China). The miR-302b-3p mimics (UAAGUGCUUCCAUGUUUUAGUAG) and control NC mimic (UUCUCCGAACGUGUCACGUTT) were also provided by GenePharma. XWLC and NCI-H292 cells were transfected with the RNA oligoribonucleotides with Lipofectamine RNAiMAX (Invitrogen, Carlsbad, CA) and Opti-MEM (Gibco, Carlsbad, CA) according to the manufacturer's recommendations. Cells were then incubated for 48h before further functional assays.

Cell proliferation assays

Cell proliferation was measured using Cell Counting Kit-8 (CCK-8) Assay kit (Dojindo, Kusatsu, Japan). The transfected cells were respectively seeded into 96-well plates (Corning Costar, Corning, NY) at a density of 3.0×10^3/ well/100 μL, and incubated in a water-saturated carbon dioxide incubator. CCK8 solution (10μl) was added to each well at 37°C for 1h, and the absorbance in each well was measured at a wavelength of 450 nm with the Thermo Scientific Multiskan FC microplate reader. Measurements of cell proliferation were performed at 24, 48, and 72 hours after transfection. All experiments were performed in triplicate. For the colony assay, cell transfection was performed 48h later as described above. Cells were then placed into 6-cm cell culture dishes at a density of 3000 cells per dish, and incubated for 10 days with medium changed every 3 days. The culture dishes were washed with phosphate buffer saline (PBS), fixed with 4% paraformaldehyde, stained with 0.25% crystal violet and counted. Colony-forming rates were then analyzed.

Cell migration and invasion assays

Cell migration and invasion assays were performed using 24-well Transwell chambers with 8-μm pores filters (Corning Costar, NY). Thirty-six hours after transfection, cells were serum starved for 12 hours, digested with trypsin, and resuspended in serum free medium. For the migration assay, a total of 10×10^4 cells in 200μL serum-free medium were seeded into the upper chambers of Transwell plates. For the invasion assay, the same numbers of cells were placed into the upper chamber of a well coated with Matrigel (BD Biosciences, San Jose, CA). The lower chambers were filed with 800μl of medium with 20% fetal bovine serum as a chemoattractant. After incubation at 37°C with 5% CO_2 for 48h, non-migratory cells were removed from the upper surface of the filter with cottons swabs, while migrated cells on the lower surface of the filter were fixed in 4% paraformaldehyde and stained with Giemsa. The numbers of migrating or invading cells were counted in 5 randomly selected fields under a microscope (Olympus, Tokyo). All experiments were performed in triplicate.

Flow cytometric analysis for cell cycle and apoptosis

Cells were harvested and washed with PBS 48 hours after transfection. For the cell cycle analysis, cells were fixed with ice-cold 70% ethanol at 4°C overnight. The fixed cells were washed with PBS, incubated with ribonuclease A (BD Biosciences) at 37°C for 30 min, and stained with propidium iodide (PI, BD Biosciences) for 30 min. DNA content was analyzed on a flow cytometer (BD FACSJazz flow cytometer, BD Biosciences). The percentages of the cells in G0–G1, S, and G2–M phases were assessed with Flowjo7.61 (Tree Star Inc., Ashland, OR), and the difference between each group was compared. For the apoptosis assays, the transfected cells were double stained with FITC-Annexin V and PI by using FITC Annexin V Apoptosis Detection Kit (BD Biosciences) according to the protocols. The stained cells were analyzed by BD FACSJazz flow cytometer (BD Biosciences), and the data was analyzed using Cell Quest software (BD Biosciences). The percentages of apoptotic cells were counted and compared between each group. All measurements were repeated in triplicate.

Table 2. Top10 up regulated mRNAs in NSCLC tissues. FC: fold change

Probe Name	Gene Symbol	FC	p value	Regulation
A_23_P7313	SPP1	46.956165	3.69E-05	up
A_23_P420209	GCNT3	29.967876	7.99E-06	up
A_24_P271696	XAGE1A	18.952316	0.017209224	up
A_33_P3296846	TMPRSS4	12.052328	4.42E-06	up
A_23_P214079	SPINK1	11.88815	0.027974647	up
A_23_P1173	HABP2	9.549286	0.007018475	up
A_23_P428298	UNC5CL	9.12929	4.10E-06	up
A_33_P3266780	PODXL2	8.74888	1.62E-05	up
A_23_P127978	B3GNT6	7.3433123	0.01715378	up
A_23_P121695	CXCL13	7.149576	0.023294007	up

Table 3. All GCNT3 probes used in mi-RIP

Probe name	Primer Sequence (5'-3')
p GCNT3 1	GAAGGGAAGGTTCTCTTTCC
p GCNT3 2	ATTCAACTGAAATCAAGTGC
p GCNT3 3	CTAGGGTTAGGGGTGAGAGA
p GCNT3 4	AAAGGATGCCACGAATTGCA
p GCNT3 5	TCTCATAGTGTGTCTCAAAG
p GCNT3 6	TGTTGGCCAACAGGTGATGG
p GCNT3 7	AGCACCCTTATCGATGTCTC
p GCNT3 8	CCAGGCATCCACCGTGCACG
p GCNT3 9	TCAAAACATGTTGGACGAAA
p GCNT3 10	GTGTAATGTGTCTCTCACTA
Probe(Control)	TTCTCCGAACGTGTCACGT

miRIP assay

The following experiments were performed as described previously [14]. The probes are listed in the Table 3. Cells were transfected with the biotin-tagged specific probe or control probe and harvested 24 h after transfection. Cells were crosslinked by formaldehyde, equilibrated in glycine buffer and scraped with lysis buffer. Cell samples were sonicated and centrifuged. The supernatant was transferred to a 2 mL tube and 50 µl was separately saved for input analysis. The supernatant lysates were incubated with M-280 beads for 1h with rotating. The beads-sample mixture was washed and incubated to reverse the formaldehyde cross-links. Subsequently, RNAs were re-purified by TRIzol. Multiplex miRNA array was used to analyze the sequences of 184 miRNAs simultaneously from a single RT-PCR reaction to discover the miRNAs that would target GCNT3 in XWLC cells.

Western blot

Total protein was extracted using lysis buffer (Biomiga, Inc, San Diego) supplemented with protease inhibitor cocktail (Roche, Mannheim, Germany) and phosphatase inhibitor cocktail (Roche), quantified using the bicinchoninic acid (BCA) method, and denatured with called sodium dodecyl sulfate polyacrylamide gel electrophoresis (SDS-PAGE) sample buffer (Takara). Protein samples (15 µg) were separated by 10% SDS-PAGE, and transferred onto polyvinylidene difluoride (PVDF, 0.20µm) membranes (Millipore, Bedford, MA). The membranes were blocked with blocking buffer (5% skim milk or bovine serum albumin in Tris-buffered saline with Tween 20) and then incubated with appropriate primary antibodies namely, GCNT3 (ab77726, 1:1000, Abcam, Cambridge, UK), E-cadherin (ab15148, 1:500, Abcam, Cambridge, UK), N-cadherin (ab18203, 1:1000, Abcam, Cambridge, UK), vimentin (ab137321, 1:3000, Abcam, Cambridge, UK), Cyclin D1 (ab134175, 1:1000, Abcam, Cambridge, UK), Erk1/2 (ab17942, 1:1000, Abcam, Cambridge, UK), p-Erk

(ab76299, 1:5000, Abcam, Cambridge, UK), β-Tubulin (MA5-16308, 1:5000, Invitrogen) overnight at 4°C. The membranes were washed for 10min three times with TBST and subsequently incubated with the corresponding secondary antibody (1:5000, Santa Cruz Biotechnology, Santa Cruz, CA) for 1 h at room temperature. Membranes were then washed another three times for 10 min each with TBST. Protein bands were visualized using Super Signal electrochemiluminescence (#34580, Thermo Scientific) and quantitated with image Pro Plus 6.0, and the data were normalized to β-tubulin loading controls. All analyses were performed at least three times.

Dual-luciferase reporter assay

The oligonucleotides in the 3' untranslated region (UTR) of the human GCNT3 harboring a putative miR-302b-3p target binding sequences was synthesized by GenePharm (Shanghai, China). As an NC, oligonucleotides containing a mutated miR-302b-3p targeting site, which was created by replacing target binding sequences with complementary bases, were also designed. The restriction enzyme cleavage sites of SacI and XhoI in the multiple cloning site (MCS) of the GP-miRGLO dual-luciferase miRNA target expression vector (Promega) were chosen as cloning sites. The wild-type and mutant 3'UTR oligonucleotides were subcloned into the downstream of the firefly luciferase gene using GP-miRGLO vector (Promega) to generate the GP-miRGLO-GCNT3-wild-type and GP-miRGLO-GCNT3-mutant, following the manufacturer's instructions. The recombinant plasmids were extracted by Pure YieldTM Plasmid Midiprep kit (Promega) and sequenced (Sain Biological Corporation, Shanghai).

For the luciferase reporter assay, 293T cells were seeded in a 24-well plate the day before transfection. The cells were co-transfected with 2μg of the recombinant plasmids (wild-type or mutant GCNT3-3'UTR) and 50nM miRNA mimics (miR-302b-3p or NC) per well. At 24 and 48 h after co-transfection, cell lysates were collected, and luciferase activities were detected using a Dual-Luciferase Reporter System (Promega).

Statistical analysis

All statistical analyses were performed using GraphPad Prism 5.0 (GraphPad software, La Jolla, CA) and SPSS version 19.0 (SPSS, Inc., Chicago, IL). Continuous variables between two groups were estimated by the Student's t-test. The relationship between GCNT3 protein expression in the IHC test and the clinicopathological factors (for categorical data) was calculated using the Chi-square test. Kaplan-Meier survival analyses were performed in 92 cases of specimens with lower or higher GCNT3 expression, and the difference was analyzed by the log-rank test. For each test, a two-sided P value < 0.05 was considered to indicate a statistically significant difference. *, **, and *** indicate statistical significance at P values of 0.05, 0.01 and 0.001, respectively.

Results

Differentially expressed mRNAs in NSCLC tissues

We performed a human gene expression microarray on 15 pairs of NSCLC and adjacent non-cancerous lung tissues. Differential expression of genes was identified by fold changes as well as P values calculated with the t-test. Since the threshold had been set for up-regulated and down-regulated genes at a fold change ≥ 2.0 and a P value < 0.05, a total of 623 up-regulated and 2118 down-regulated mRNAs were identified in NSCLC samples compared with adjacent normal lung tissues by Student's t-test method, as depicted in the volcano plot (Fig. 1A) and the heat map (Fig. 1B). Among them, SPP1 [19], GCNT3 [11], TMPRSS4[20], SPINK1 [21], HABP2 [22], and CXCL13 [23] are known oncogenes for tumor i-genesis, while two, namely TMPRSS4 and HABP2, were identified as oncogenes in lung cancer. The top 10 up-regulated mRNAs in NSCLC tissues are listed in Table 2. We selected GCNT3 for the subsequent analysis.

GCNT3 expression was upregulated in NSCLC specimens, and high expression of GCNT3 correlated with poor prognosis in NSCLC patients.

To investigate the role of GCNT3 in the tumorigenesis of NSCLC, we firstly examined the expression of GCNT3 in NSCLC tissues. In Fig. 1C, 15 pairs of NSCLC and adjacent non-cancerous tissues had markedly increased levels of GCNT3 mRNA in NSCLC tissues compared with adjacent non-cancerous tissues by real-time PCR ($P < 0.001$). Similar results were observed after re-analyzing gene expression data in 226 NSCLC tissues and 20 normal tissues downloaded from The Cancer Genome Atlas (TCGA: https://tcga-data.nci.nih.gov/docs/publications/tcga/), a public dataset with clinical information and mRNA expression levels of all patients at the Oncomine website (https://www.oncomine.org) (Fig. 1D). Taken together, these results indicated that GCNT3 might play a critical role in the progression of NSCLC.

We then evaluated GCNT3 expression in 92 pairs of NSCLC and adjacent non-cancerous tissues using IHC staining. The results indicated that GCNT3 was highly increased in NSCLC tissues at the protein level (Fig. 1E-1F). Furthermore, according to IHC, we divided the 92 NSCLC patients into a high GCNT3 expression group (above average GCNT3 expression, n = 55) and a low expression group (below average GCNT3 expression, n = 37). As presented in Table 1, we explored the clinical significance of GCNT3 in NSCLC, and the correlation between GCNT3 expression levels and the patients' clinical features were analyzed by the Chi-square test. The results implied that the expression of GCNT3 was closely associated with TNM stage ($P = 0.0078$), lymph node metastasis ($P = 0.0016$), and survival years after surgery ($P = 0.0033$). Nevertheless, there was no correlation between the expression level of GCNT3 and age, sex or tumor size (all $P > 0.05$). The correlation between the expression of GCNT3 protein and prognosis in NSCLC patients was assessed by Kaplan-Meier survival curves and a log-rank test. The results showed that higher expression of GCNT3 correlated with shorter OS among NSCLC patients ($P = 0.042$, Fig. 1G). The P value was assessed by the log-rank test.

Knockdown of GCNT3 inhibited NSCLC cell proliferation, migration, and invasion, and induced cell cycle arrest and apoptosis.

To further investigate the biological function of GCNT3 in NSCLC, we detected the expression of GCNT3 in four human NSCLC cell lines (A549, GLC, XWLC and NCI-H292) and a human Normal pulmonary epithelial cell line (BEAS-2B). As illustrated in Fig. 2A, XWLC and NCI-H292 cells exhibited higher expression of GCNT3 at the protein level. Thus, we knocked down endogenous GCNT3 expression by siRNA transfection in XWLC and NCI-H292 cells (Fig. 2B). After GCNT3 knockdown, growth curves detected by CCK8 assay implied that the proliferative ability of both XWLC and NCI-H292 cells was remarkably inhibited (all $P < 0.05$, Fig. 2C). Furthermore, the colony formation assay indicated that the colony formation rates of GCNT3-knockdown XWLC and NCI-H292 cells were much lower than those transfected with siNC (Fig. 2D). These data indicated that downregulation of GCNT3 repressed the proliferation of NSCLC cells.

A flow cytometry assay was conducted to identify the stages of cell cycle progression in XWLC and NCI-H292 cells transfected with GCNT3-siRNA or NC-si. The results indicated that GCNT3-siRNA transfection in XWLC and NCI-H292 cells led to a remarkable increase in the percentages of cells at G0/G1 phase and a marked decrease in cells at S phase. G2/M phase was not obviously affected after downregulation of GCNT3. (all $P < 0.01$, Fig. S1A - for all supplemental material see www.karger.com/10.1159/000494482/) To investigate the potential mechanisms underlying the suppression of growth after GCNT3 downregulation, annexin V-FITC/PI staining assay was performed to assess the effect on NSCLC cell apoptosis. The results revealed that the percentage of cells in early apoptosis in XWLC-siGCNT3 and NCI-H292-GCNT3 was higher than that in XWLC-NC ($P < 0.01$) and NCI-H292-NC ($P < 0.01$),

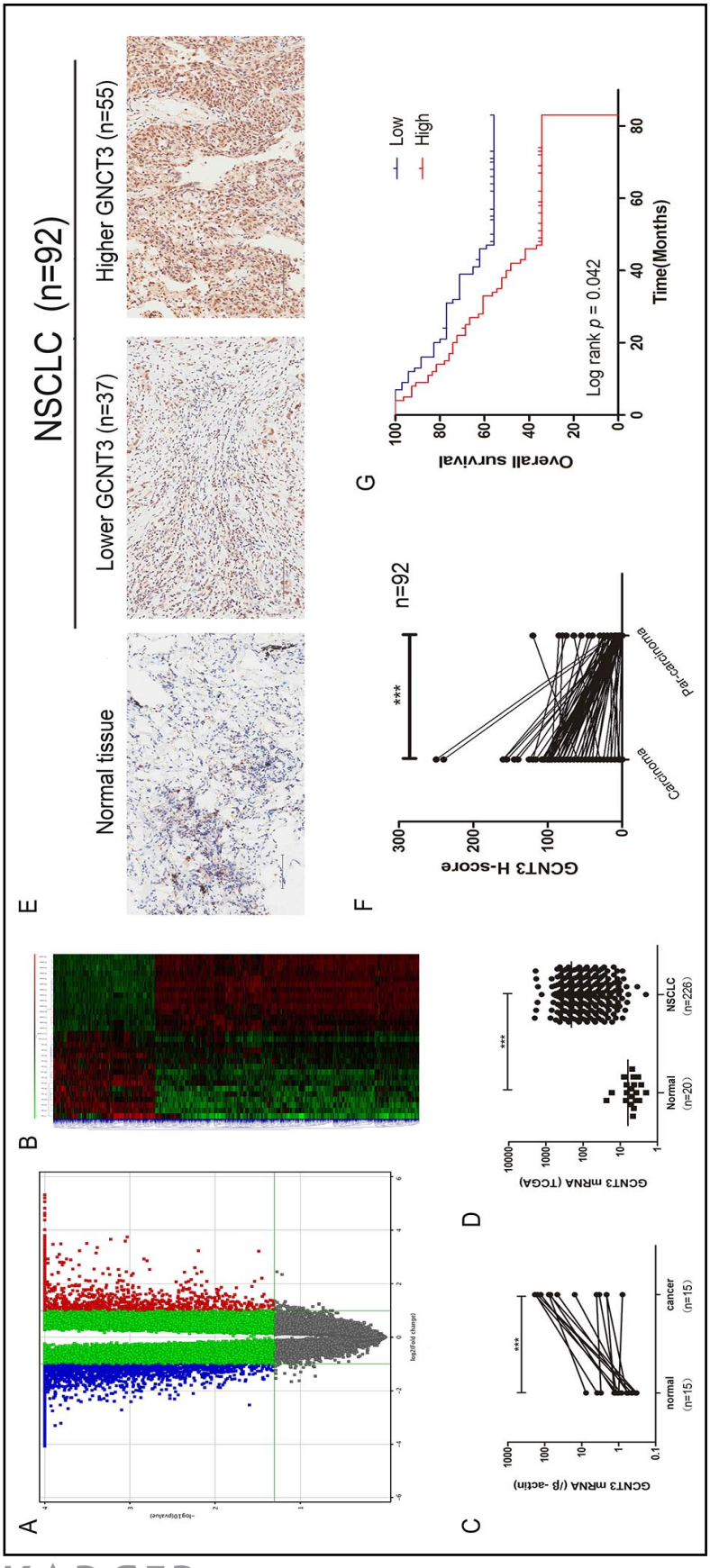

Fig. 1. GCNT3 was overexpressed in NSCLC, and its high expression was involved with poor prognosis. (A) Volcano plot of P values as a function of the weighted fold change for mRNAs in NSCLC tissues. (B) Heatmap of expression profiles for the 2741 mRNAs showed significant expression changes (623 up-regulated and 2118 down-regulated). (C) mRNA levels of GCNT3 were examined in 15 pairs NSCLC tissues and noncancerous tissues by qPCR, and normalized to GAPDH expression (P<0.001). (D) GCNT3 expression in NSCLC and normal tissues based on TCGA dataset (P<0.001). (E) The protein expression in NSCLC tissues and adjacent noncancerous tissues was assessed by immunohistochemistry assay. (F) GCNT3 was upregulated in Carcinoma tissues compared to the Par-carcinoma tissues, determined by IHC assay (P<0.001). (G) Kaplan-Meier survival analysis showed that the overall survival of NSCLC patients with higher GCNT3 expression was significantly shorter than those with lower GCNT3 expression (P<0.05; Scale bar: 100 μm).

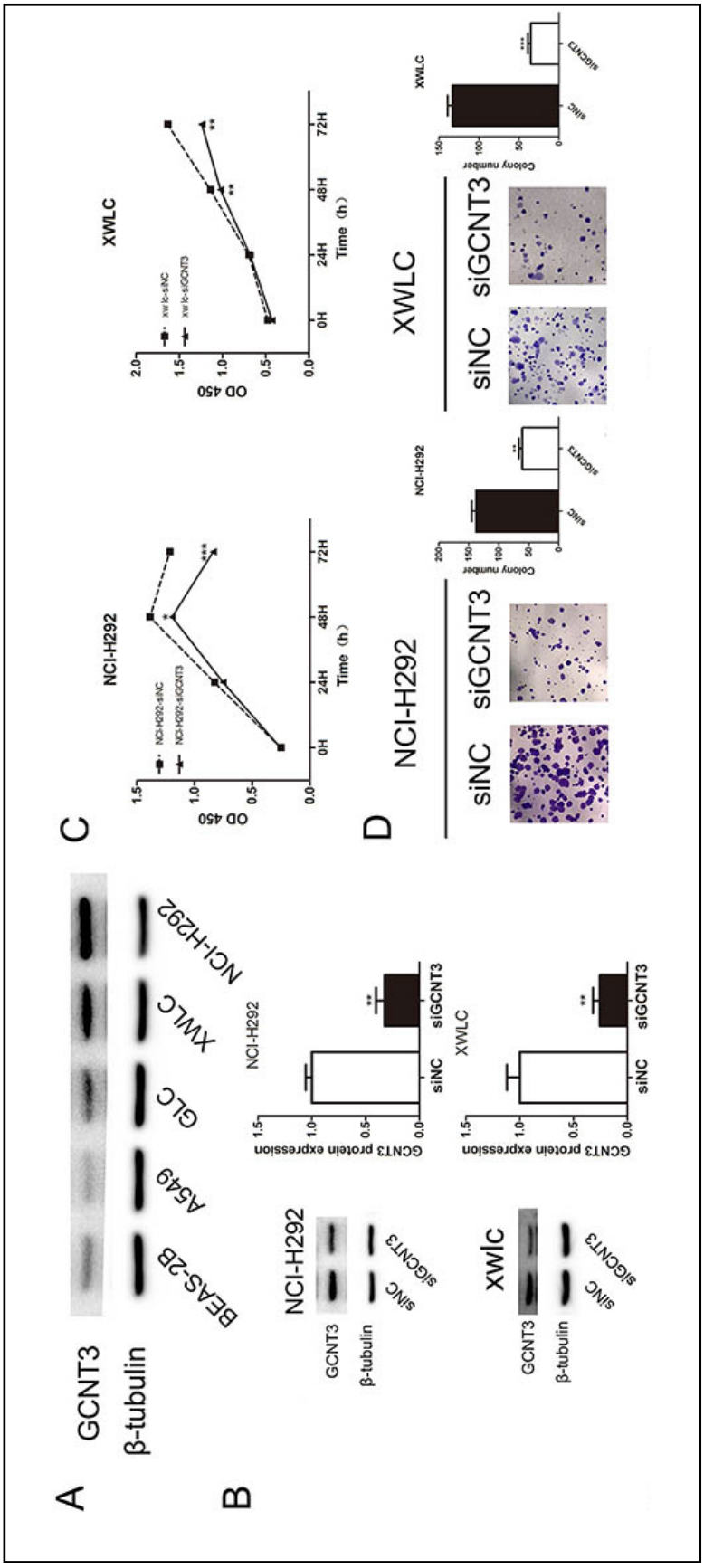

Fig. 2. GCNT3 protein levels in NSCLC cell lines, and GCNT3 knockdown inhibited NSCLC cell proliferation. (A) Western blot assay showing GCNT3 protein levels in four human NSCLC cell lines (A549, GLC, XWLC and NCI-H292) and a human Normal pulmonary epithelial cell line (BEAS-2B). (B) Western blot below suggesting significant knockdown of GCNT3 mediated by siRNA after 48hours post-transfection in two NSCLC cell lines (XWLC and NCI-H292). β-tubulin was used as the loading control. (C) CCK8 assay was performed to measure the proliferation of XWLC and NCI-H292 cell lines at 0, 24, 48 and 72 h after siRNA and siNC (control) transfection. (D) Colony-forming assay was used to detect the proliferation of si-GCNT3-transfected XWLC and NCI-H292 cell lines. Data was based on at least 3 independent experiments, and shown as mean ± SD. (*P<0.05; **P<0.01; ***P<0.001).

and the percentage of cells in late apoptosis in XWLC-siGCNT3 and NCI-H292-GCNT3 was also higher than in XWLC-NC ($P < 0.01$) and NCI-H292-NC ($P < 0.05$). These results indicated that the inhibition of GCNT3 expression promoted apoptosis in NSCLC cells, which suggested that GCNT3 contributed to tumor progression by inhibiting apoptosis (Fig. S1B).

Since the metastasis of cancer cells is known to be a crucial indicator of tumor progression, we detected the migration and invasion capacities of NSCLC cells after transfecting them with siGCNT3 or siNC via transwell assays with non-Matrigel-coated and Matrigel coated inserts, respectively. As shown in Fig. S1D and 3E, GCNT3 knockdown clearly repressed the migration and invasion capacities of XWLC and NCI-H292 cells (all $P < 0.01$).

To investigate the regulatory mechanism of GCNT3, we detected certain vital proteins that might be involved in EMT, cell cycle progression and the Erk pathways. As shown in Fig. S1C, western blotting assay showed that the protein levels of cyclin D1, N-cadherin, vimentin and p-Erk (phosphorylation of Erk) were downregulated, while thoses of E-caderherin were markedly increased, after GCNT3 knockdown. However, the levels of Erk protein showed no significant change. These data suggested that GCNT3 could regulate migration, invasion, the cell cycle and Erk pathway associated proteins.

GCNT3 overexpression promoted proliferation, migration and invasion in NSCLC cells

To further unravel the function of GCNT3 in the oncogenesis of NSCLC, GCNT3 was significantly upregulated in XWLC and NCI-H292 cells by GCNT3 plasmid transfection. The colony formation assay results suggested that upregulation of GCNT3 expression enhanced colony forming abilities in XWLC and NCI-H292 cells (Fig. S2B-C, $P < 0.05$). Tumor migration (Fig. S2D) and invasion (Fig. S2E) were also enhanced by transfecting GCNT3 plasmid into XWLC and NCI-H292 cells. We detected a couple of proteins that might be involved with the Erk signaling pathways and EMT. Western blotting indicated that the protein levels of N-cadherin, vimentin and p-Erk were upregulated, while the level of E-cadherin was markedly decreased, after GCNT3 overexpression (Fig. S2A).

miR-302b-3p directly targeted the GCNT3, and regulated NSCLC tumor progression

miRNAs can regulate a broad range of cellular processes through post-translational modulation of their targets [13]. To understand the mechanism by which GCNT3 affected NSCLC progression risk after miRNA, the miRIP method was used to identify the miRNAs targeting GCNT3 [14]. Ten probes of GCNT3 were transfected into XWLC cells to hybridize with GCNT3 mRNA for 24 h (Fig. S3A). The associated mRNAs of GCNT3 were purified using Streptavidin Dynabeads (M-280) and isolated by TRIzol. Multiplex miRNA array was used to analyze the sequences of 184 miRNAs simultaneously from a single RT-PCR reaction to discover the associated miRNAs targeting GCNT3 in XWLC cells. miR-302b-3p, interacted with GCNT3 mRNA robustly, was selected for further investigation (Fig. S3B). We then detected the expression of miR-302b-3p in four human NSCLC cell lines (A549, GLC, XWLC and NCI-H292) and a human normal pulmonary epithelial cell line (BEAS-2B). As illustrated in Fig. S3C, XWLC and NCI-H292 cells exhibited lower expression of miR-302b-3p. These results indicated that miR-302b-3p correlated negatively with GCNT3 in NSCLC cell lines.

To further investigate the function of miR-302b-3p in NSCLC cells, we transfected a miR-302b-3p mimic into XWLC and NCI-H292 cells. As illustrated in Fig. S3D, miR-302b-3p overexpression inhibited GCNT3 expression at the protein level in XWLC and NCI-H292 cells. After transfection with miR-302b-3p, growth curves detected by the CCK-8 assay implied that the proliferative ability of XWLC and NCI-H292 cells was remarkably inhibited (all $P < 0.05$, Fig. S3E). Tumor migration (Fig. S3F) and invasion (Fig. S3G) activities were also suppressed by transfection with miR-302b-3p in XWLC and NCI-H292 cells. Our data suggested that miR-302b-3p directly targeted GCNT3 and was involved in tumorigenesis in NSCLC.

To confirm whether GCNT3 gene was a direct target of miR-302b-3p, a dual luciferase reporter assay was performed in 293T cells. We first performed a bioinformatics analysis using Miranda (http://34.236.212.39/microrna/home.do) to find out the putative miR-302b-3p target binding sequences in the 3'UTR of the human GCNT3. (Fig. 3A) The partial

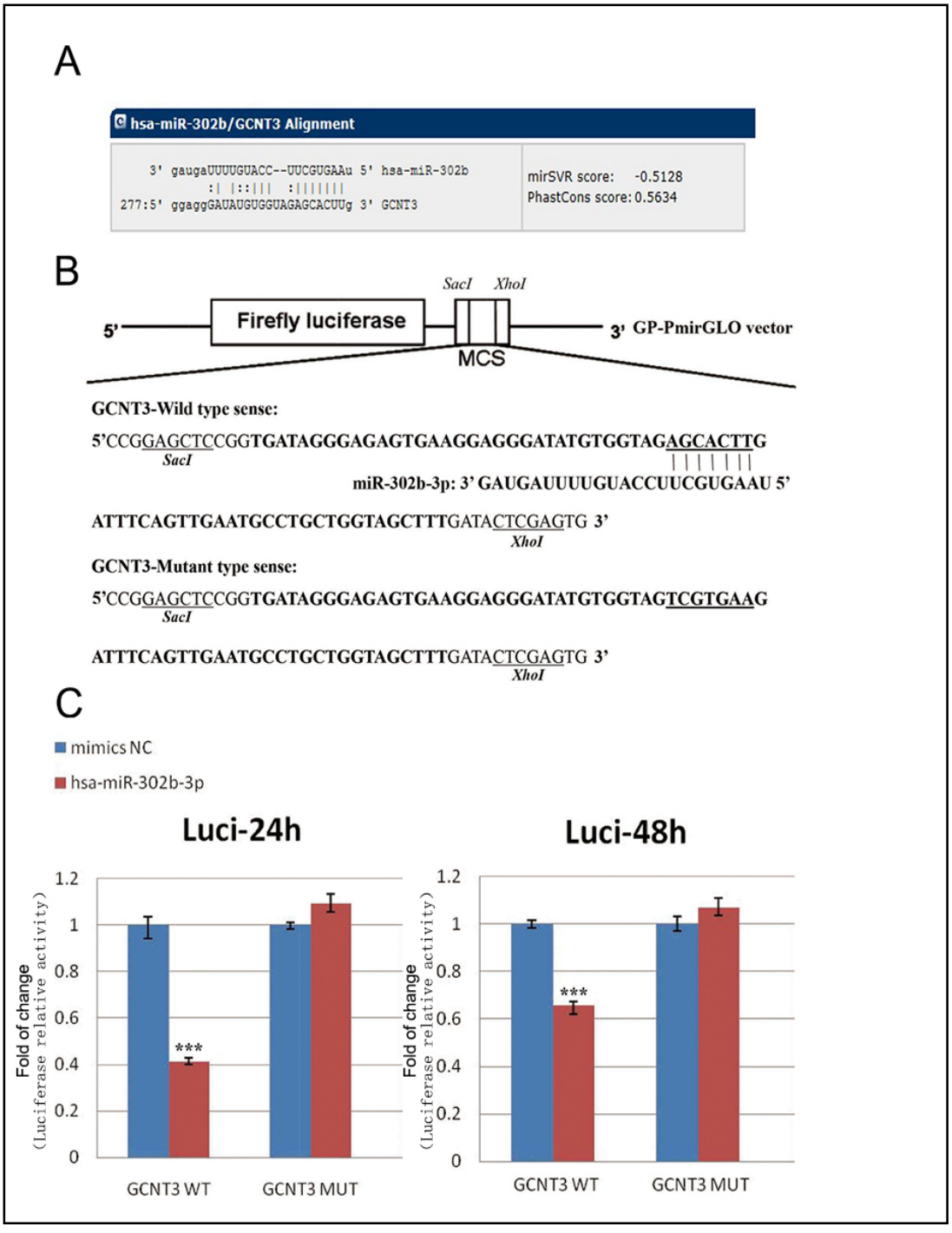

Fig. 3. miR-302b-3p was found to be the GCNT3-binding miRNA through dual luciferase reporter gene assays. (A) The putative miR-302b-3p target binding sequences in the 3'UTR of the human GCNT3 predicted by bioinformatics analysis was listed below. (B) The GCNT3-wild-type with putative binding site of miR-302b-3p and the mutant generated by replacing the binding region of miR-302b-3p with complementary bases were subcloned into the GP-miRGLO vector, respectively. The restriction enzyme cutting sites of the SacI and XhoI were chosen as the cloning sites. (C) For luciferase assay, the cells were co-transfected with 2ug of the recombinant plasmids (WT or mutant GCNT3-3'UTR) and 50nM miRNA mimics (miR-302b-3p or NC) per well. Luciferase activities were measured twenty-four and forty-eight hours after transfection. Firefly luciferase activities were normalized by the activity of renilla luciferase. The experiments were performed in triplicate. (*P<0.05; **P<0.01; ***P<0.001).

sequence in the 3'UTR of the human GCNT3 harboring putative miR-302b-3p target binding sequences was synthesized. As an NC, a fragment with the same part of GCNT3 3'UTR with the miR-302b-3p binding site replaced by complementary bases was also synthesized. These two fragments were subcloned into a dual-luciferase reportor vector to generate the GP-miRGLO-GCNT3-wild-type and GP-miRGLO-GCNT3-mutant. (Fig. 3B) The miRNA (miR-302b-3p or NC mimics, 50nM) and the recombinant plasmids (GP-miRGLO-GCNT3-wild-type or GP-miRGLO-GCNT3-mutant, 2μg) were co-transfected into 293T cells for 24 h and 48 h. The results indicated that miR-302b-3p strongly inhibited the activity of the firefly luciferase gene of the reporter vector containing the GCNT3 3'UTR with a wild-type miR-302b-3p binding site, but did not inhibit the reporter vector with mutant GCNT3 3'UTR (Fig. 3C). This result indicated that miR-302b-3p inhibited the expression of GCNT3 by directly targeting the 3'UTR.

miR-302b-3p overexpression suppressed NSCLC cell proliferation, migration and invasion in a GCNT3-dependent manner

We found that GCNT3 was the target of miR-302b-3p, and facilitated NSCLC progression. Thus, rescue experiment was conducted to identify whether GCNT3 overexpression could reverse the phenotype of miR-302b-3p overexpression. The colony formation assay results revealed that the overexpression of miR-302b-3p suppressed colony formting abilities in XWLC and NCI-H292 cells (Fig. S4B, $P < 0.05$), while miR-302b-3p and GCNT3 co-overexpression reversed the miR-302b-3p overexpression-induced decline in colony forming abilities (Fig. S4B). The transwell assay with or without Matrigel suggested that miR-302b-3p overexpression markedly inhibited migration and invasion in NSCLC cells, while miR-302b-3p and GCNT3 co-overexpression restored these abilities compared with miR-302b-3p overexpression. (Fig. S4C and D, $P < 0.01$) In addition, we examined the expression of some proteins regulated by the Erk signaling pathway and EMT. Western blot results revealed that the overexpression of miR-302b-3p downregulated the protein levels of GCNT3, N-cadherin, vimentin, and p-Erk and elevated the levels of E-cadherin. In contrast, co-transfection with miR-302b-3p and GCNT3 abrogated the effects of miR-302b-3p on the levels of these proteins (Fig. S4A).

Discussion

Epidemiological studies [4-6] indicate that XWLC has peculiar traits, such as high rates of incidence and death, low male-to-female ratio, younger age at onset, and adenocarcinoma as the dominant type. Strong evidence revealed that XWLC is a special type of adenocarcinoma caused by indoor air pollution from household burning of solid fuels, which contain carcinogenics polycyclic aromatic hydrocarbons [24, 25]. Thereby, it is essential to clarify the pathogenetic mechanisms in this kind of lung cancer in the Xuanwei area to enable early detection, and prognostic and therapeutic strategies. In this study, differential expression of mRNAs was screened through mRNA microarray between NSCLC tissues and matched adjacent non-cancerous lung tissues from the patients in Xuanwei, Yunnan Province, China. We focused on GCNT3, because when it is up-regulated, it has been found to be associated with clinical indexes in patients with NSCLC. Knockdown of GCNT3 inhibited the proliferation, migration and invasion ability of NSCLC cells, while GCNT3 overexpression promoted these activities. Furthermore, GCNT3 was a target of miR-302b-3p as confirmed in miRIP and dual luciferase reporter gene assays. Overexpression of miR-302b-3p inhibited cell proliferation, migration and invasion by suppressing GCNT3 expression, while miR-302b-3p and GCNT3 co-overexpression reversed the miR-302b-3p overexpression phenotype. In addition, western blotting revealed that E-cadherin, N-cadherin, vimentin, cyclin D1 and p-Erk were downstream molecules of the miR-302b-3p/GCNT3 pathway.

GCNT3 is a member of the N-acetylglucosaminyltransferase family involved in mucin biosynthesis [8]. Abnormal expression of GCNT3 promotes the formation of mucins to enhance

the flexibility of cancer cells and allow them to adapt to adverse tumor microenvironment conditions [9-12]. Analysis of clinical data from NSCLC patients and expression data from TCGA indicated that GCNT3 was up-regulated in NSCLC tissues and associated with TNM stage, lymph node metastasis and patients' OS (Table 1 and Fig. 1). In addition, GNCT3 was also over-expressed in NSCLC cells compared with normal cells (Fig. 2). The GCNT3 inhibition and overexpression functional assays were performed in XWLC/NCI-H292 cell lines to explore the biological roles of GCNT3 in NSCLC tumorigenesis (Fig. 2, Fig. S1 and S2). The results showed that knockdown of GCNT3 exerted tumor-suppressive effects by reducing NSCLC cell proliferation, while GCNT3 overexpression promoted tumorigenesis by facilitating NSCLC cell proliferation. Transwell assay showed that knockdown of GCNT3 in XWLC and NCI-H292 cells suppressed cell migration and invasion, while overexpression of GCNT3 in A549 cells promoted migration and invasion. These results indicated that GCNT3 could be highly related to tumorigenesis in NSCLC.

As important regulators in downstream oncogenic pathways, miRNAs have been found to contribute to oncogenesis [26]. Alterations in miRNA expression have been reported in several human tumors including those in the colon [27], prostate [28], lung [29], breast [30], liver [31], pancreas [32], and bladder [33]. The mi-RIP method was performed to precisely identify the miRNAs that can bind to the GCNT3 mRNA in NSCLC cells [14]. miR-302b-3p was found to interact robustly with GCNT3 mRNA, and was selected for the next investigation. In recent studies, miR-302b has been found to be a tumor suppressor in various tumors, including esophageal cancer [34], hepatocellular carcinoma [35], and gastric cancer [36]. Zhang et al. (2017) reported that miR-302b decreased esophageal cancer growth by targeting ERBB4, IRF2 and CXCR4 and inhibiting CRI critical pathway and expression of downstream cytokines [34]. Wang et al. (2016) identified that miR-302b inhibited human hepatocellular carcinoma cell metastasis and invasion by targeting the AKT2/NF-kB/MMP-2 pathway [35]. In addition, miR-302b was also found to target and negatively regulate the expression of CDK2 to decrease cell proliferation and arrest the cell cycle in gastric cancer tissues by suppressing the Erk signal pathway [36]. In the present study, miR-302b-3p was found to be the GCNT3-binding miRNA through miRIP and dual luciferase reporter gene assays (Fig. S3 and Fig. 3). It was significantly down-regulated in NSCLC cell lines. The results also showed that overexpression of miR-320b-3p down-regulated the expression of GCNT3 and decreased the proliferation, migration and invasion abilities of NSCLC cells. (Fig. S3) The rescue assay showed that these effects could be abrogated by re-expression of GCNT3, indicating that miR-302b-3p acted as a repressor of NSCLC cells in a GCNT3-dependent manner. In addition, miR-302b-3p overexpression remarkably inhibited NCI-H292 cell proliferation after incubation for 24h, whereas the inhibition of cell proliferation by si-GCNT3 was revealed in NCI-H292 48 h after incubation. (Fig. S4) The reason for these results is that miR-302b not only inhibited the expression of GCNT3, but also modulated the expression of its target genes, such as ERBB4, IRF2, CXCR4 [34], AKT2/NF-kB/MMP-2 pathway [35], CDK2 [36], ErbB4 et al. [37], and AKT2 [38]. As we know, one single miRNA can regulate a broad range of cellular processes including cell growth, proliferation and apoptosis, by post-translational modulation of the target genes [13]. Therefore, the overexpression of miR-302b-3p might be more effective than down-regulation of GCNT3 in inhibiting the proliferation of NSCLC cells.

Recent evidence has shown that GCNT3 promotes human tumorigenesis [9, 10], and the EMT process has been confirmed to be an essential process for tumor invasion and metastasis [39]. E-cadherin [40], N-cadherin [41] and vimentin [42] have been identified as the main factors in the EMT process. In the present study, we revealed that knockdown of GCNT3 expression or restoration of miR-302b-3p can suppress the migratory and invasive phenotype in XWLC and NCI-H292 cells, and increase the level of E-cadherin, while decreasing the expression of N-cadherin and vimentin. These results suggested that GCNT3 and miR-302b-3p affect NSCLC metastasis partly via the EMT. In addition, the Erk signaling pathway has been shown to be frequently activated in numerous kinds of human cancers [43-45]. Aberrant activation of phosphorylated Erk1/2 induced by miRNAs has been observed in lung cancer [45-47]. Recent reports point out that miR-379 acts as a tumor

suppressor in NSCLC by indirectly regulation of ERK signaling pathways [45], miR-7 inhibits the activation of ERK/MAPK signaling pathway by down-regulating FAK expression [46], and miR-622 overexpression decreases invasion in lung tumor cells by inhibiting HIF-1alpha via inactivation of ERK signaling in A549 cell [47]. Consistent with these findings, we found that the p-Erk level was significantly decreased in response to GCNT3 silencing or miR-302b-3p overexpression in XWLC and NCI-H292 cells, suggesting that the effect of the miR-302b-3p/GCNT3 signaling pathway in NSCLC may depend on the activation of p-Erk. Moreover, we investigated potential targets that could be responsible for GCNT3 mediated cell cycle arrest. In this study, the expression of cyclin D1 was significantly decreased in GCNT3-knockdown XWLC and NCI-H292 cells, which was consistent with the results of cell cycle analysis. Cyclin D1 is a well-established cell cycle regulatory protein, involved in the pathogenesis of several human tumor types, including lung cancer, breast cancer and pancreatic cancer [48-50]. Cyclin D1 controls cell cycle transition from the G1 to S phase, which is essential for the dividing cell to enter the DNA synthesis phase [51]. Thus, we speculated that GCNT3 could positively regulate cell cycle progression in NSCLC by altering the expression of cyclin D1. All together, these findings indicated that E-cadherin, N-cadherin, vimentin, cyclin D1 and Erk were the downstream factors of the axis of miR-302b-3p/GCNT3.

In conclusion, GCNT3 was regarded as an oncogene in NSCLC, and a target of miR-302b-3p, which regulated cell proliferation, migration and invasion in a GCNT3-dependent manner. Moreover, E-cadherin, N-cadherin, vimentin, cyclin D1 and p-Erk appeared to be downstream molecules of the miR-302b-3p/GCNT3 pathway.

Conclusion

Taken together, the miR-302b-3p/GCNT3 pathway may participate in the initiation and progression of NSCLC, and may be an important cancer promoter and novel candidate for NSCLC therapy.

Acknowledgements

We are grateful to all the patients participating in this study. This work was financially supported by the grants from the National Natural Science Foundation of China (No.81860499 to CJ. Xiao and No.81460435, No. 81860494 to SY. Zheng), and the Academic young scholar of distinction for doctoral post graduate in Yunnan province (C6155501).

Disclosure Statement

The authors declare that they have no conflict of interest.

References

1 Jemal A, Siegel R, Ward E, Hao Y, Xu J, Thun MJ: Cancer statistics, 2009. CA Cancer J Clin 2009;59:225-249.
2 Torre LA, Bray F, Siegel RL, Ferlay J, Lortet-Tieulent J, Jemal A: Global cancer statistics, 2012. CA Cancer J Clin 2015;65:87-108.
3 Siegel R, Naishadham D, Jemal A: Cancer statistics, 2013. CA Cancer J Clin 2013;63:11-30.
4 Wang D, He X, Liu Y: Risk factors of lung cancer and relevant comprehensive preventive strategy--a cohort study in Xuanwei, Yunnan Province, China. Zhonghua Yi Xue Za Zhi 2001;81:876-880.
5 Xiao Y, Shao Y, Yu X, Zhou G: The epidemic status and risk factors of lung cancer in Xuanwei City, Yunnan Province, China. Front Med 2012;6:388-394.

6 Liu L, Wan X, Chen G, Ma X, Ning B, Yang G: Risk Factors of Lung Cancer in Xuanwei, Yunnan Province, China. Chinese journal of lung cancer 2017;20:528-537.
7 Verdecchia A, Francisci S, Brenner H, Gatta G, Micheli A, Mangone L, Kunkler I: Recent cancer survival in Europe: a 2000-02 period analysis of EUROCARE-4 data. Lancet Oncol 2007;8:784-796.
8 Li RW, Li C, Elsasser TH, Liu G, Garrett WM, Gasbarre LC: Mucin biosynthesis in the bovine goblet cell induced by Cooperia oncophora infection. Vet Parasitol 2009;165:281-289.
9 Rao CV, Janakiram NB, Mohammed A: Molecular Pathways: Mucins and Drug Delivery in Cancer. Clin Cancer Res 2017;23:1373-1378.
10 Rao CV, Janakiram NB, Madka V, Kumar G, Scott EJ, Pathuri G, Bryant T, Kutche H, Zhang Y, Biddick L, Gali H, Zhao YD, Lightfoot S, Mohammed A: Small-Molecule Inhibition of GCNT3 Disrupts Mucin Biosynthesis and Malignant Cellular Behaviors in Pancreatic Cancer. Cancer Res 2016;76:1965-1974.
11 Gonzalez-Vallinas M, Vargas T, Moreno-Rubio J, Molina S, Herranz J, Cejas P, Burgos E, Aguayo C, Custodio A, Reglero G, Feliu J, Ramirez de Molina A: Clinical relevance of the differential expression of the glycosyltransferase gene GCNT3 in colon cancer. Eur J Cancer 2015;51:1-8.
12 Iwano S, Ichikawa M, Takizawa S, Hashimoto H, Miyamoto Y: Identification of AhR-regulated genes involved in PAH-induced immunotoxicity using a highly-sensitive DNA chip, 3D-Gene Human Immunity and Metabolic Syndrome 9k. Toxicol *In vitro* 2010;24:85-91.
13 Baltimore D, Boldin MP, O'Connell RM, Rao DS, Taganov KD: MicroRNAs: new regulators of immune cell development and function. Nat Immunol 2008;9:839-845.
14 Su X, Wang H, Ge W, Yang M, Hou J, Chen T, Li N, Cao X: An *In vivo* Method to Identify microRNA Targets Not Predicted by Computation Algorithms: p21 Targeting by miR-92a in Cancer. Cancer Res 2015;75:2875-2885.
15 Cataldo A, Cheung DG, Balsari A, Tagliabue E, Coppola V, Iorio MV, Palmieri D, Croce CM: miR-302b enhances breast cancer cell sensitivity to cisplatin by regulating E2F1 and the cellular DNA damage response. Oncotarget 2016;7:786-797.
16 Wang L, Yao J, Shi X, Hu L, Li Z, Song T, Huang C: MicroRNA-302b suppresses cell proliferation by targeting EGFR in human hepatocellular carcinoma SMMC-7721 cells. BMC Cancer 2013;13:448.
17 Ge T, Yin M, Yang M, Liu T, Lou G: MicroRNA-302b suppresses human epithelial ovarian cancer cell growth by targeting RUNX1. Cell Physiol Biochem 2014;34:2209-2220.
18 Goldstraw P: Updated staging system for lung cancer. Surg Oncol Clin N Am 2011;20:655-666.
19 Xu C, Sun L, Jiang C, Zhou H, Gu L, Liu Y, Xu Q: SPP1, analyzed by bioinformatics methods, promotes the metastasis in colorectal cancer by activating EMT pathway. Biomed Pharmacother 2017;91:1167-1177.
20 Villalba M, Diaz-Lagares A, Redrado M, de Aberasturi AL, Segura V, Bodegas ME, Pajares MJ, Pio R, Freire J, Gomez-Roman J, Montuenga LM, Esteller M, Sandoval J, Calvo A: Epigenetic alterations leading to TMPRSS4 promoter hypomethylation and protein overexpression predict poor prognosis in squamous lung cancer patients. Oncotarget 2016;7:22752-22769.
21 Huang KC, Evans A, Donnelly B, Bismar TA: SPINK1 Overexpression in Localized Prostate Cancer: a Rare Event Inversely Associated with ERG Expression and Exclusive of Homozygous PTEN Deletion. Pathol Oncol Res 2017;23:399-407.
22 Mirzapoiazova T, Mambetsariev N, Lennon FE, Mambetsariev B, Berlind JE, Salgia R, Singleton PA: HABP2 is a Novel Regulator of Hyaluronan-Mediated Human Lung Cancer Progression. Front Oncol 2015;5:164.
23 Fan L, Zhu Q, Liu L, Zhu C, Huang H, Lu S, Liu P: CXCL13 is androgen-responsive and involved in androgen induced prostate cancer cell migration and invasion. Oncotarget 2017;8:53244-53261.
24 Lv J, Xu R, Wu G, Zhang Q, Li Y, Wang P, Liao C, Liu J, Jiang G, Wei F: Indoor and outdoor air pollution of polycyclic aromatic hydrocarbons (PAHs) in Xuanwei and Fuyuan, China. J Environ Monit 2009;11:1368-1374.
25 Mumford JL, Helmes CT, Lee XM, Seidenberg J, Nesnow S: Mouse skin tumorigenicity studies of indoor coal and wood combustion emissions from homes of residents in Xuan Wei, China with high lung cancer mortality. Carcinogenesis 1990;11:397-403.
26 Garzon R, Calin GA, Croce CM: MicroRNAs in Cancer. Annu Rev Med 2009;60:167-179.
27 Schepeler T, Reinert JT, Ostenfeld MS, Christensen LL, Silahtaroglu AN, Dyrskjot L, Wiuf C, Sorensen FJ, Kruhoffer M, Laurberg S, Kauppinen S, Orntoft TF, Andersen CL: Diagnostic and prognostic microRNAs in stage II colon cancer. Cancer Res 2008;68:6416-6424.

28 Ozen M, Creighton CJ, Ozdemir M, Ittmann M: Widespread deregulation of microRNA expression in human prostate cancer. Oncogene 2008;27:1788-1793.
29 Yanaihara N, Caplen N, Bowman E, Seike M, Kumamoto K, Yi M, Stephens RM, Okamoto A, Yokota J, Tanaka T, Calin GA, Liu CG, Croce CM, Harris CC: Unique microRNA molecular profiles in lung cancer diagnosis and prognosis. Cancer Cell 2006;9:189-198.
30 Blenkiron C, Goldstein LD, Thorne NP, Spiteri I, Chin SF, Dunning MJ, Barbosa-Morais NL, Teschendorff AE, Green AR, Ellis IO, Tavare S, Caldas C, Miska EA: MicroRNA expression profiling of human breast cancer identifies new markers of tumor subtype. Genome Biol 2007;8:R214.
31 Murakami Y, Yasuda T, Saigo K, Urashima T, Toyoda H, Okanoue T, Shimotohno K: Comprehensive analysis of microRNA expression patterns in hepatocellular carcinoma and non-tumorous tissues. Oncogene 2006;25:2537-2545.
32 Bloomston M, Frankel WL, Petrocca F, Volinia S, Alder H, Hagan JP, Liu CG, Bhatt D, Taccioli C, Croce CM: MicroRNA expression patterns to differentiate pancreatic adenocarcinoma from normal pancreas and chronic pancreatitis. JAMA 2007;297:1901-1908.
33 Gottardo F, Liu CG, Ferracin M, Calin GA, Fassan M, Bassi P, Sevignani C, Byrne D, Negrini M, Pagano F, Gomella LG, Croce CM, Baffa R: Micro-RNA profiling in kidney and bladder cancers. Urol Oncol 2007;25:387-392.
34 Zhang M, Zhang L, Cui M, Ye W, Zhang P, Zhou S, Wang J: miR-302b inhibits cancer-related inflammation by targeting ERBB4, IRF2 and CXCR4 in esophageal cancer. Oncotarget 2017;8:49053-49063.
35 Wang L, Yao J, Sun H, Sun R, Chang S, Yang Y, Song T, Huang C: miR-302b suppresses cell invasion and metastasis by directly targeting AKT2 in human hepatocellular carcinoma cells. Tumour Biol 2016;37:847-855.
36 Liu FY, Wang LP, Wang Q, Han P, Zhuang WP, Li MJ, Yuan H: miR-302b regulates cell cycles by targeting CDK2 via ERK signaling pathway in gastric cancer. Cancer Med 2016;5:2302-2313.
37 Zhang M, Yang Q, Zhang L, Zhou S, Ye W, Yao Q, Li Z, Huang C, Wen Q, Wang J: miR-302b is a potential molecular marker of esophageal squamous cell carcinoma and functions as a tumor suppressor by targeting ErbB4. J Exp Clin Cancer Res 2014;33:10.
38 Wang L, Yao J, Zhang X, Guo B, Le X, Cubberly M, Li Z, Nan K, Song T, Huang C: miRNA-302b suppresses human hepatocellular carcinoma by targeting AKT2. Mol Cancer Res 2014;12:190-202.
39 Xie M, Nie FQ, Sun M, Xia R, Liu YW, Zhou P, De W, Liu XH: Decreased long noncoding RNA SPRY4-IT1 contributing to gastric cancer cell metastasis partly via affecting epithelial-mesenchymal transition. J Transl Med 2015;13:250.
40 Bindels EM, Vermey M, van den Beemd R, Dinjens WN, Van Der Kwast TH: E-cadherin promotes intraepithelial expansion of bladder carcinoma cells in an *in vitro* model of carcinoma in situ. Cancer Res 2000;60:177-183.
41 Sarrio D, Rodriguez-Pinilla SM, Hardisson D, Cano A, Moreno-Bueno G, Palacios J: Epithelial-mesenchymal transition in breast cancer relates to the basal-like phenotype. Cancer Res 2008;68:989-997.
42 Maier J, Traenkle B, Rothbauer U: Visualizing Epithelial-Mesenchymal Transition Using the Chromobody Technology. Cancer Res 2016;76:5592-5596.
43 Senmaru N, Shichinohe T, Takeuchi M, Miyamoto M, Sazawa A, Ogiso Y, Takahashi T, Okushiba S, Takimoto M, Kato H, Kuzumaki N: Suppression of Erk activation and *in vivo* growth in esophageal cancer cells by the dominant negative Ras mutant, N116Y. Int J Cancer 1998;78:366-371.
44 Nguyen TT, Tran E, Nguyen TH, Do PT, Huynh TH, Huynh H: The role of activated MEK-ERK pathway in quercetin-induced growth inhibition and apoptosis in A549 lung cancer cells. Carcinogenesis 2004;25:647-659.
45 Zhou F, Nie L, Feng D, Guo S, Luo R: MicroRNA-379 acts as a tumor suppressor in non-small cell lung cancer by targeting the IGF1R-mediated AKT and ERK pathways. Oncol Rep 2017;38:1857-1866.
46 Cao Q, Mao ZD, Shi YJ, Chen Y, Sun Y, Zhang Q, Song L, Peng LP: MicroRNA-7 inhibits cell proliferation, migration and invasion in human non-small cell lung cancer cells by targeting FAK through ERK/MAPK signaling pathway. Oncotarget 2016;7:77468-77481.
47 Cheng CW, Chen PM, Hsieh YH, Weng CC, Chang CW, Yao CC, Hu LY, Wu PE, Shen CY: Foxo3a-mediated overexpression of microRNA-622 suppresses tumor metastasis by repressing hypoxia-inducible factor-1alpha in ERK-responsive lung cancer. Oncotarget 2015;6:44222-44238.

48 Gautschi O, Ratschiller D, Gugger M, Betticher DC, Heighway J: Cyclin D1 in non-small cell lung cancer: a key driver of malignant transformation. Lung Cancer 2007;55:1-14.
49 Yu Q, Geng Y, Sicinski P: Specific protection against breast cancers by cyclin D1 ablation. Nature 2001;411:1017-1021.
50 Kornmann M, Ishiwata T, Itakura J, Tangvoranuntakul P, Beger HG, Korc M: Increased cyclin D1 in human pancreatic cancer is associated with decreased postoperative survival. Oncology 1998;55:363-369.
51 Todd R, Hinds PW, Munger K, Rustgi AK, Opitz OG, Suliman Y, Wong DT: Cell cycle dysregulation in oral cancer. Crit Rev Oral Biol Med 2002;13:51-61.